Electronic Supplementary Material (ESI) for Analyst.

Supplementary Material - Manipulating the insulating post arrangement in DC-biased AC-iEK devices to improve microparticle separations

Nuzhet Nihaar Nasir Ahamed[a], Carlos A. Mendiola-Escobedo[b], Victor H. Perez-Gonzalez[b,*] and Blanca H. Lapizco-Encinas[a,*]

[a] Microscale Bioseparations Laboratory and Biomedical Engineering Department, Rochester Institute of Technology, 160 Lomb Memorial Drive, Rochester, New York, 14623, United States.

[b] School of Engineering and Sciences, Tecnologico de Monterrey, Monterrey, Nuevo Leon 64849, Mexico.

Correspondence should be addressed to the following authors:
Victor H. Perez-Gonzalez (PhD)
Email: vhpg@tec.mx

Blanca H. Lapizco-Encinas (PhD)
Email: bhlbme@rit.edu

CONTENTS

Nonlinear electrophoretic velocity evaluation in the moderate field regime: includes Table S1

The dependence of the electrophoretic velocity on the electric field strength was analyzed for the system used in this study by using the following parameters - the dimensionless applied electric field magnitude, and the Dukhin and Peclet numbers.[1–3] The dimensionless field strength coefficient (β) is deemed as the ratio of the applied electric field magnitude (E) multiplied by the particle radius (a) to the thermal voltage (φ_T):

$$\beta = \frac{Ea}{\varphi_T} \tag{S1}$$

The *Dukhin* number (*Du*) describes the ratio of the surface conductivity (K^σ) of the microparticle to the bulk conductivity (K_m) of the electrolyte suspending medium times the particle radius, and it is defined as follows:

$$Du = \frac{K^\sigma}{K_m a} \tag{S2}$$

The *Peclet* number (*Pe*) describes the ratio of convective transport to the diffusive transport of the electrolyte ions that are close to the microparticle surface, and it is calculated as follows:

$$Pe = \frac{a|(v_{EP,L} + v_{EP,NL})|}{D} \tag{S3}$$

where $v_{EP,L}$ and $v_{EP,NL}$ refers to the linear and nonlinear electrophoretic particle velocity, respectively, and D is the diffusion coefficient.

Table S1. Values of the parameters used for investigating the moderate field regime representing cubic dependence (E^3).

Particle ID	β	*Du*	*Pe*	E for estimating parameters (V/cm)	Dependence of nonlinear EP with E
Particle 1-Red	1.3	0.02	0.3	100	Moderate E^3
Particle 2-Green	1.3	0.03	0.5	100	Moderate E^3

Computational model information: includes Figure S1, and Table S2

COMSOL Multiphysics was employed to build a 2D computational model to estimate the electric field distribution across the device. The velocity components exhibited by the particles because of each of the four EK phenomena were also simulated. Furthermore, the overall particle velocity and the predicted retention time of the particles across the post array were predicted. This 2D model is an appropriate choice for the modeling because the changes along the depth of the channel can be neglected.[4] The Electric Currents module within COMSOL Multiphysics was used to solve the Laplace equation in a time-dependent study. The deviation of the predicted retention times ($t_{R,p}$) vs. experimental retention times ($t_{R,e}$) for each particle was evaluated to calculate the model precision. All material properties used in this model were acquired from the COMSOL Material Library, the conductivity and relative permittivity (ε_r) of the fluid suspending medium were set to 4.07 x 10^{-3} S/m (40.7 µS/cm) and 78.4, respectively. **Figure S1** illustrates domain and boundary conditions used in the computational model, and **Table S2** shows these conditions as equations. Maximum and minimum element sizes for free triangular meshes were 130 µm and 0.261 µm, respectively.

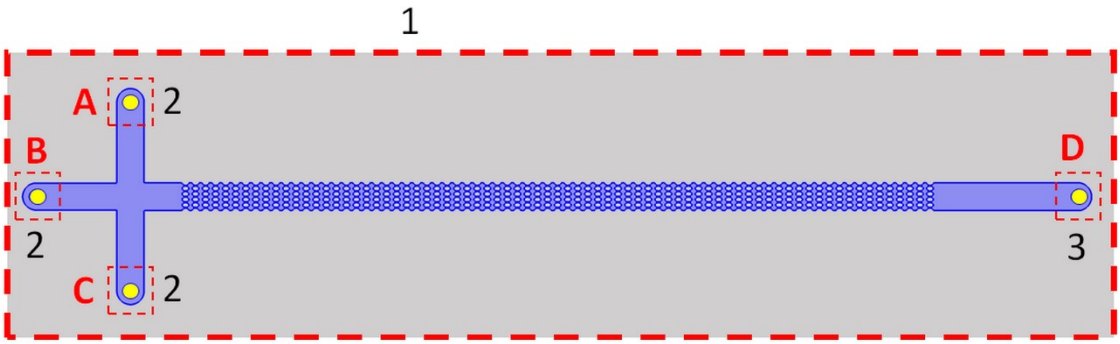

Figure S1. Depiction of the domains and boundaries used in the computational model where gray color shows the PDMS domain, the blue color illustrates the fluid suspending medium domain, and the yellow color indicates the platinum electrodes. The labels A, B, C, and D, indicate the electrodes for the EK injection process, as illustrated in **Table 2** of the manuscript. Device dimensions are shown in **Figure 1** in the manuscript. The dashed red boxes correspond to the boundaries, which are represented by the numbers 1,2 and 3, used in the computational model. Boundary 1 represents the outer PDMS surface; boundary 2 describes the three reservoirs where electric potentials are applied: A, B, and C. Boundary 3 is the ground electrode D, all boundary conditions are itemized in **Table S2**.

Table S2. Computational model information, comprising domain and boundary conditions. Device dimensions are shown in **Figure 1** in the manuscript. Domains are displayed in **Fig. S1**.

Domain conditions		
Domain type	**Element region & color**	**Definition***
Current conservation	PDMS domain (channel walls and insulating posts), gray color Fluid suspending medium domain, blue color Platinum electrodes domain, yellow color	$\nabla \cdot J = -\nabla \cdot \left(\left(\sigma + \varepsilon_0 \varepsilon_r \frac{\partial}{\partial t}\right) E\right)$; where $E = -\nabla V$
Initial values	PDMS domain (channel walls and insulating posts), gray color Fluid suspending medium domain, blue color Platinum electrodes domain, yellow color	$V_0 = 0$
Boundary conditions		
Boundary condition type	**Element number**	**Definition**
Electric insulation	1	$n \cdot J = 0$
Electric potential	2	$V_A = V_{applied,A}$; $V_B(t) = V_{DC} + V_p \sin(\omega t)$; $V_C = V_{applied,C}$; $V_D = V_{applied,D}$;

*V represents the electric potential, J is the electric current density vector, n is the normal unit vector, $\omega = 2\pi f$, with f the AC frequency, and V_p is the peak amplitude of the applied AC electric potential. The variables ε_0 and ε_r represent the permittivity of the vacuum and the relative permittivity of each given domain, respectively. The permittivity of a given domain is $\varepsilon = \varepsilon_0 \varepsilon_r$.

Characteristics of the 12 distinct device designs: includes Table S3

Table S3 lists all the geometrical characteristics of the post arrays in the 12 distinct device designs employed in this work.

Table S3. Dimensions of the spacing between the insulating posts (HS and VS), values of the spacing between posts normalized to particle diameter (NHS and NVS), and description of the type of post arrangement for each of12 distinct device designs used in this study.

Device ID and post arrangement	Device design				
	Horizontal spacing, HS (μm)	Normalized horizontal spacing, NHS (dimensionless)	Vertical spacing, VS (μm)	Normalized vertical spacing, NVS (dimensionless)	Post arrangement
1 HS-75 VS-35	75	15	35	7	Square
2 HS-105 VS-35	105	21	35	7	Square
3 HS-135 VS-35	135	27	35	7	Square
4 HS-75 VS-18	75	15	18	3.6	Square
5 HS-105 VS-18	105	21	18	3.6	Square
6 HS-135 VS-18	135	27	18	3.6	Square
7 HS-75 VS-35 OFFSET	75	15	35	7	Offset
8 HS-105 VS-35 OFFSET	105	21	35	7	Offset
9 HS-135 VS-35 OFFSET	135	27	35	7	Offset
10 HS-75 VS-18 OFFSET	75	15	18	3.6	Offset
11 HS-105 VS-18 OFFSET	105	21	18	3.6	Offset
12 HS-135 VS-18 OFFSET	135	27	18	3.6	Offset

Expression for flow rate: includes Table S4

A formal expression of the fluid's flow rate (Q) as function of electric field E, can be determined as follows:

$$Q = v_{EO}A \quad \text{(S4)}$$

where v_{EO} represents the electroosmotic (EO) flow velocity and A the cross-sectional area of the microchannel.

Based on Equation (1) from the manuscript, Equation (S4) can be rewritten as:

$$Q = \mu_{EO}E\,wh \quad \text{(S5)}$$

where μ_{EO}, w, and h refer to the linear EO mobility, width, and height of the microchannel, respectively.

Since a time-dependent DC-biased AC potential is applied for the separation experiments, the minimum and maximum electric field magnitude (E) in the microchannel corresponds to the minimum and maximum part of the time-dependent AC signal. The flow rate obtained during the maximum and minimum portion of the DC-biased AC signal, corresponding to the maximum and minimum values of E (E_{max} and E_{min}), for all the 12 different channel designs is given in **Table S4**.

Table S4. Values of flow rate corresponding to the minimum and maximum electric field magnitude, obtained during the application of the time-dependent DC-biased AC signal, with the 12 device designs included in this study. The value of μ_{EO} for all device designs was 4.7×10^{-8} $m^2\ V^{-1}\ s^{-1}$. The width and height for all channel designs were 1.1 mm, and 40 µm, respectively.

Device ID	E_{max} (V/cm)	E_{min} (V/cm)	Q_{max} (nL/s)	Q_{min} (nL/s)
1	39.85	-0.43	8.80	-0.09
2	44.50	-0.48	9.83	-0.11
3	51.04	-0.55	11.27	-0.12
4	56.32	-1.42	11.54	-0.29
5	62.78	-1.59	12.86	-0.33
6	72.03	-1.82	14.76	-0.37
7	26.11	-0.28	5.77	-0.06
8	29.50	-0.32	6.52	-0.07
9	32.05	-0.34	7.08	-0.08
10	46.68	-1.18	9.57	-0.24
11	52.58	-1.33	10.78	-0.27
12	59.21	-1.50	12.13	-0.31

Reproducibility between experimental repetitions: includes Table S5

Each experimental separation was performed three times, Table S5 lists the results obtained in each separation and presents the average and standard deviations of the experimental retentions times.

Table S5. Values of retention times for three distinct experimental repetitions of the separations with each one of the 12 devices included in this study.

Device ID	Particles	$t_{R,e}$ Repetition 1 (s)	$t_{R,e}$ Repetition 2 (s)	$t_{R,e}$ Repetition 3 (s)	Average (s)	Range of stdev (%)
1	Particle 1 (Red)	150	200	150	167	17

	Particle 2 (Green)	270	265	250	262	4
2	Particle 1 (Red)	181	187	191	186	3
	Particle 2 (Green)	278	278	293	283	3.1
3	Particle 1 (Red)	206	205	239	217	9
	Particle 2 (Green)	354	316	364	345	7.4
4	Particle 1 (Red)	213	196	219	209	6
	Particle 2 (Green)	390	362	373	375	4
5	Particle 1 (Red)	296	250	252	266	10
	Particle 2 (Green)	453	420	470	448	5.7
6	Particle 1 (Red)	247	285	279	270	8
	Particle 2 (Green)	444	478	509	477	6.8
7	Particle 1 (Red)	177	148	215	180	19
	Particle 2 (Green)	323	294	350	322	8.7
8	Particle 1 (Red)	208	218	230	219	5
	Particle 2 (Green)	352	387	380	374	5
9	Particle 1 (Red)	213	248	236	232	8
	Particle 2 (Green)	337	380	400	373	8.7
10	Particle 1 (Red)	268	209	223	233	13
	Particle 2 (Green)	409	433	365	402	9
11	Particle 1 (Red)	275	217	220	237	14
	Particle 2 (Green)	500	459	474	477	4
12	Particle 1 (Red)	290	266	310	289	8
	Particle 2 (Green)	542	498	518	519	4

Estimation of the predicted retention time with COMSOL model: includes Figure S2, and Figure S3

The cutlines used for predicting the overall particle velocity along the constriction between posts are depicted in **Figure S2** and **Figure S3**. For posts arranged in a square array, the cutline spanned two constrictions, and for posts arranged in an offset configuration, the cutline spanned across one constriction only. The lengths of these horizontal cutlines are specified within the figure and also in the figure caption. The total time required for each particle type to migrate across the cutline was predicted using the velocity data obtained over the cutline, then by multiplying this value by the number of columns of posts (75), it was possible to estimate the total particle retention time ($t_{R,p}$).

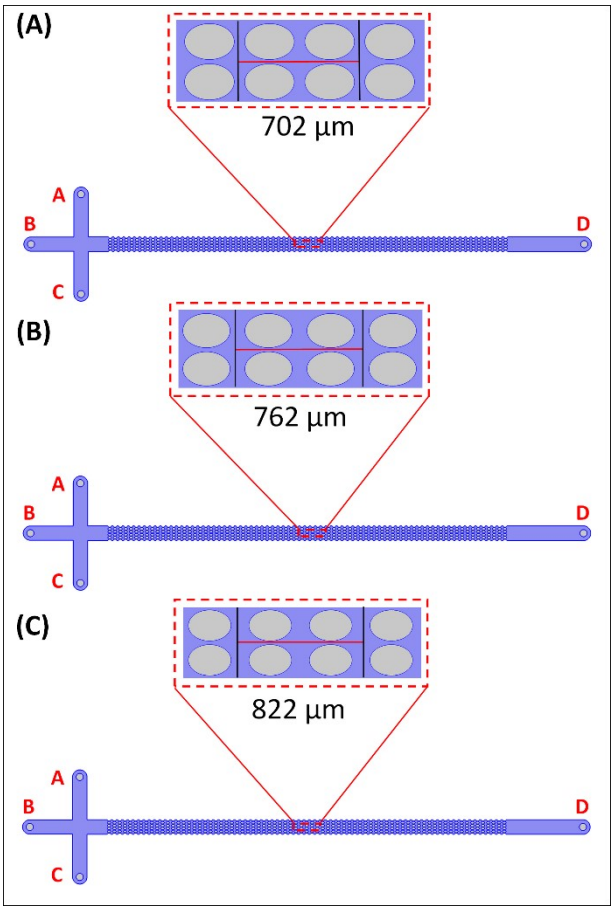

Figure S2. Representation of the cutlines defined in COMSOL Multiphysics to predict retention time for different device designs with a square post arrangement **(A)** For devices ID: 1 and 4, the total cutline length is 276 µm + 276 µm + 75 µm + 75 µm = 702 µm. **(B)** For devices ID: 2 and 5, the total cutline length is 276 µm + 276 µm + 105 µm + 105 µm = 762 µm. **(C)** For devices ID: 3 and 6, the total cutline length is 276 µm + 276 µm + 135 µm + 135 µm = 822 µm.

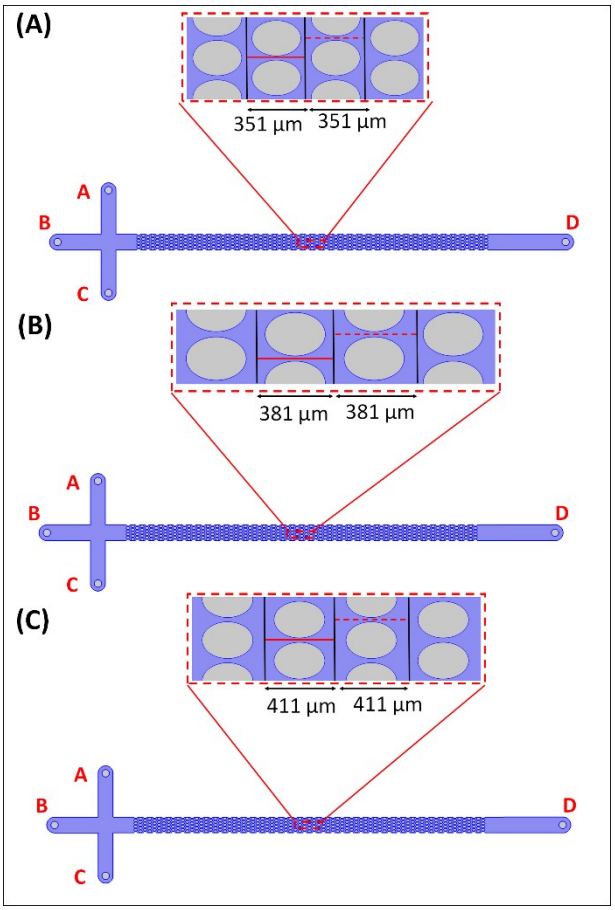

Figure S3. Representation of the cutlines defined in COMSOL Multiphysics to predict retention time for device designs with an offset post arrangement. Two cutlines for each device with an offset post arrangement are defined, where one cutline is between two non-offset posts and the other cutline is between two offset posts. **(A)** For devices ID: 7 and 10, the total cutline length is 37.5 µm + 276 µm + 37.5 µm = 351 µm. **(B)** For devices ID: 8 and 11, the total cutline length is 52.5 µm + 276 µm + 52.5 µm = 381 µm. **(C)** For devices ID: 9 and 12, the total cutline length is 67.5 µm + 276 µm + 67.5 µm = 411 µm.

Comparison of the velocity magnitudes of all four EK phenomena: includes Figures S4-S10

We employed COMSOL to predict the maximum electric field magnitude and particle velocities over the cutlines depicted in **Figure S2** and **Figure S3**. The results are shown in **Figures S4-S6**, where the effect of varying the HS and VS between posts and introducing an offset to the post array on particle velocities is investigated. Prediction of individual particle velocities as a result of each one of the four phenomena, is shown in **Figures S7-S10**, where it can be observed that the separations with all device designs is mainly in the linear EK regime since linear EO and linear EP are the main EK phenomena contributing to the overall particle velocities . Based on the predictions, it is shown that at the voltages selected (**Table 2** in the manuscript), the magnitude of the nonlinear EK effects of DEP and $EP_{NL}^{(3)}$ was kept low, thus, allowing the separation to take place by mainly exploiting linear EP effects as dictated by the particle zeta potential values (**Table 1** in the manuscript).

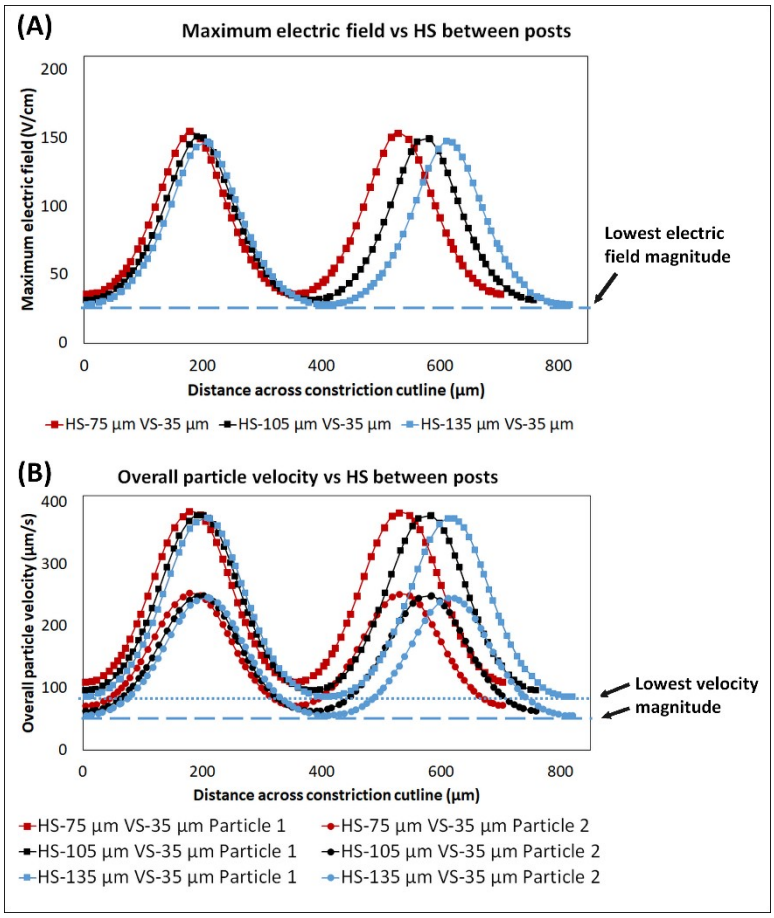

Figure S4. Prediction of the maximum electric field magnitude and overall particle velocities across a cutline for Devices ID #1, #2 and #3, where the effect of varying HS between posts was studied for devices with constant VS between posts as 35 µm. The cutlines are depicted in **Figure S2**. **(A)** The maximum electric field magnitude across the cutline for two constrictions. **(B)** Overall particle velocities for both the particles across the cutline for two constrictions.

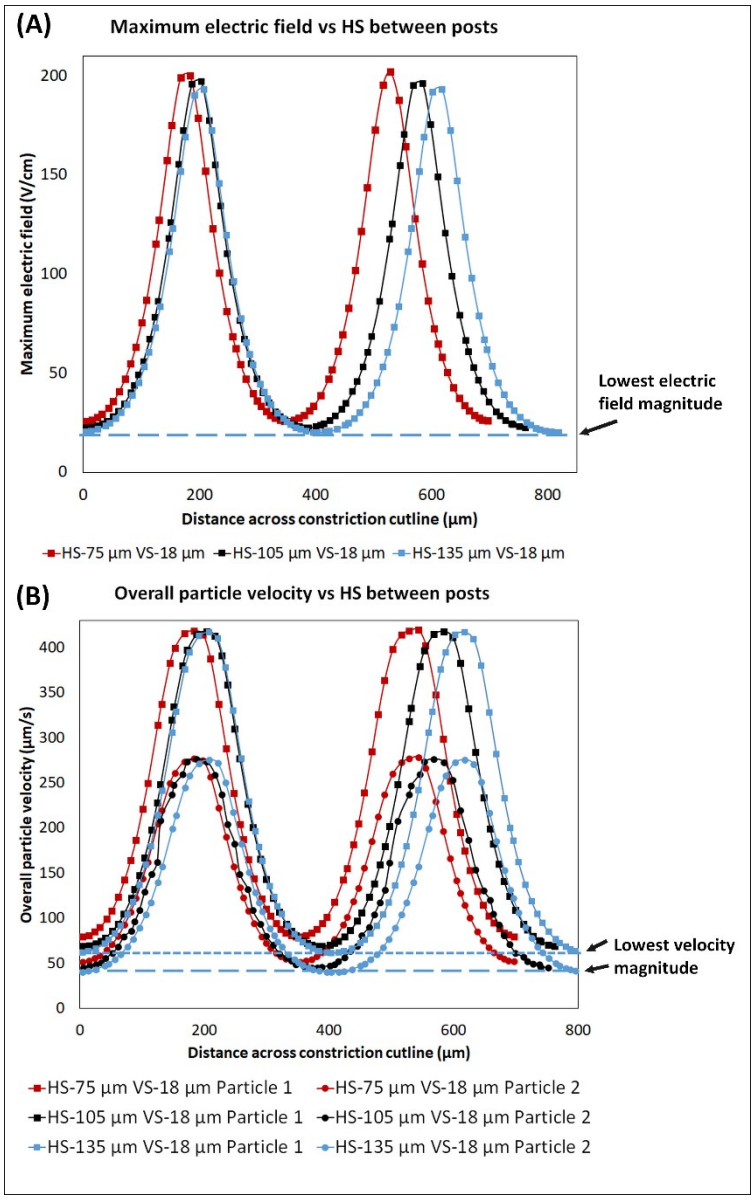

Figure S5. Prediction of the maximum electric field magnitude and overall particle velocities across a cutline for Device ID 4, 5 and 6, where the effect of varying VS between posts (as VS = 18 µm) was studied. The cutlines are depicted in **Figure S2**. **(A)** The maximum electric field magnitude versus the distance across the cutline between two constrictions for different HS between posts. **(B)** The overall particle velocities for both the particles versus the distance across the cutline for two constrictions for different HS between posts.

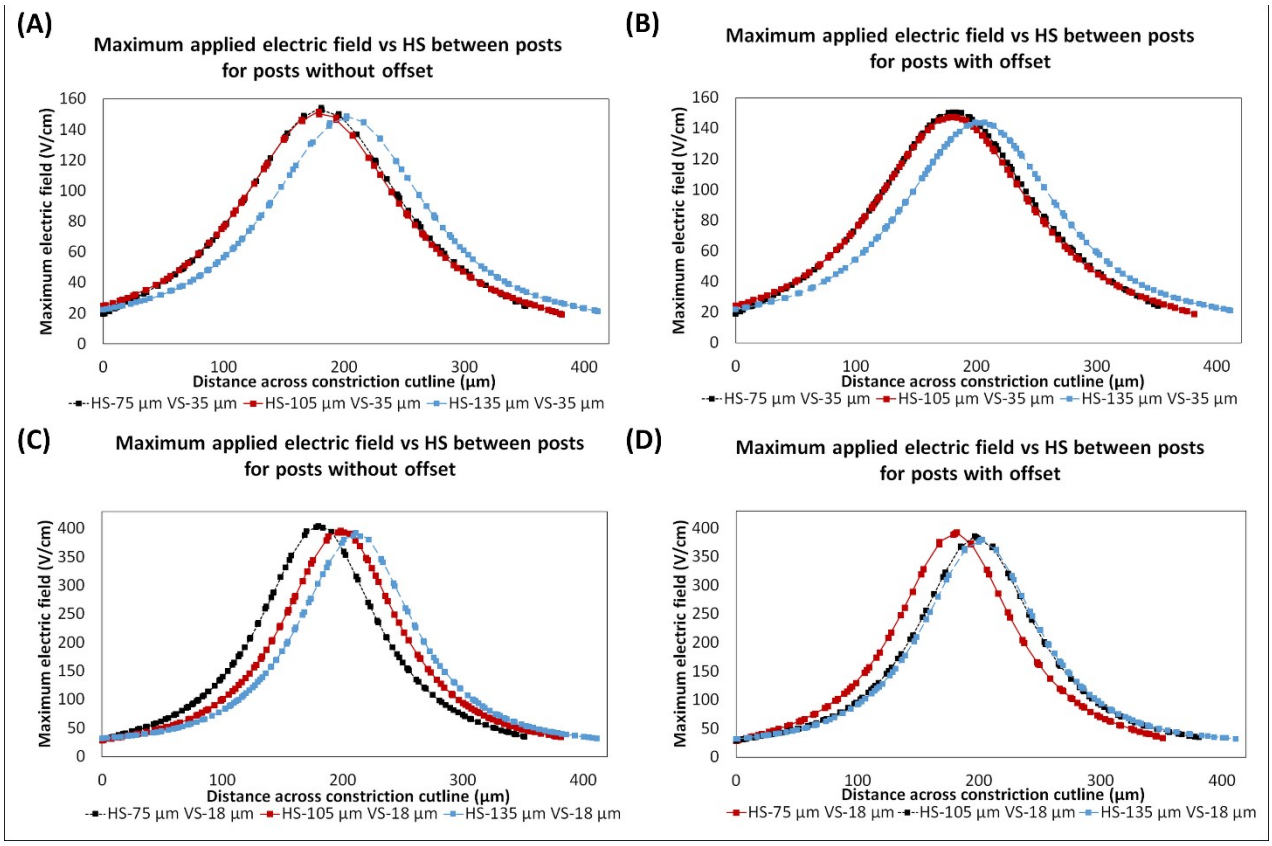

Figure S6. Prediction of the maximum electric field magnitude across the two cutlines for Device ID #7 to #12, where the effect of introducing an offset to the post array was studied. The cutlines across a post constriction between non-offset and offset posts are each depicted in **Figure S3**. **(A, B)** For Device ID #7 to #9, where VS = 35 µm, and **(C, D)** For Device ID #10 to #12, where VS=18 µm, the maximum electric field magnitude versus the distance across the cutline for one post constriction for posts without and with offset, respectively.

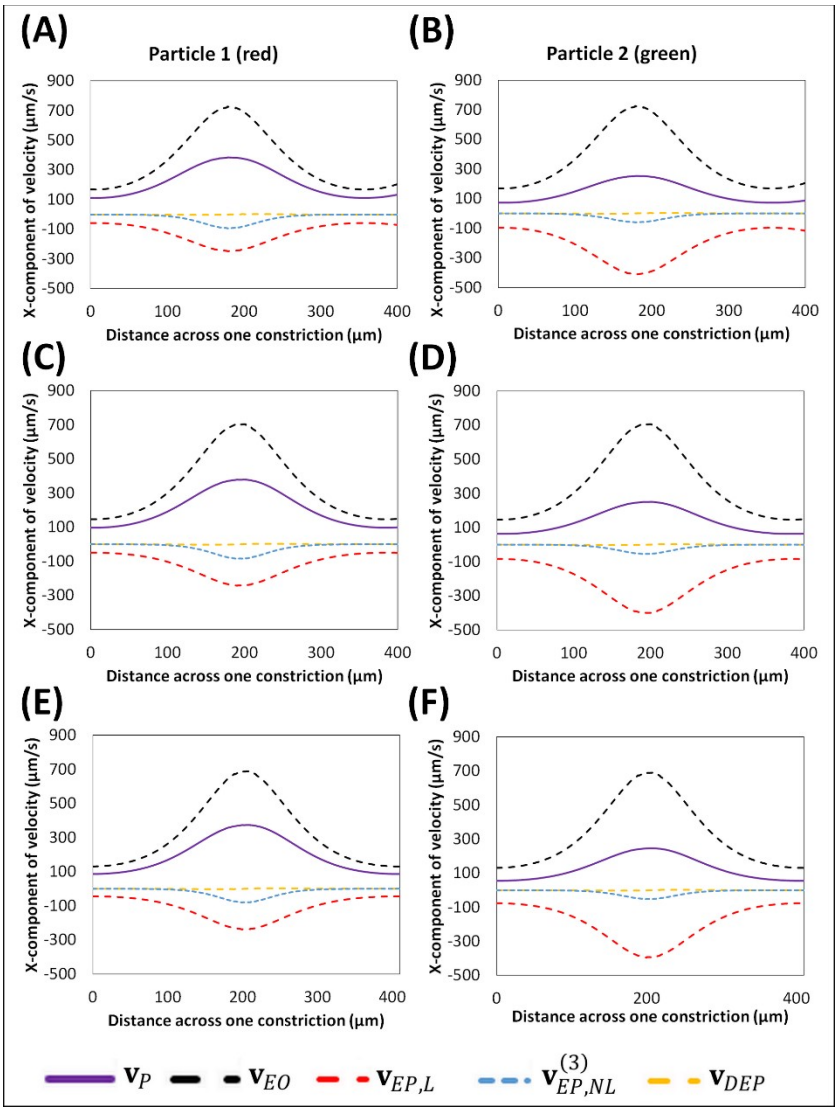

Figure S7. Prediction of the overall and individual particle velocities exerted by the four EK phenomena across a cutline for Device IDs 1-3, by varying HS , under 800 V peak amplitude and 300 V DC bias at 1.1 Hz frequency. The predicted velocities are plotted across one post constriction, along the cutline in **Figure S2**, at the maximum electric field generated by the applied AC signal for red and green particles, in (A,B) Device ID 1 (C, D) Device ID 2, and (E,F) Device ID 3, respectively.

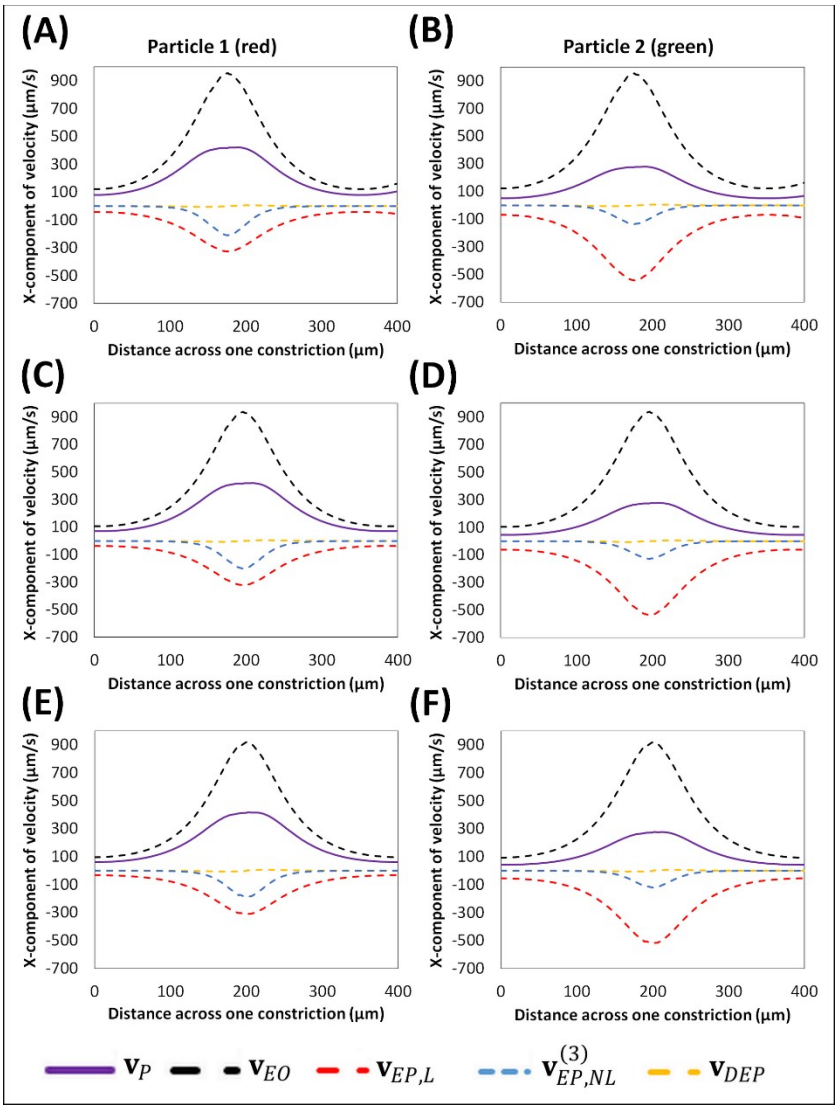

Figure S8. Prediction of the overall and individual particle velocities exerted by the four EK phenomena across a cutline for Device IDs 4-6, by varying the VS, under 800 V peak amplitude and 300 V DC bias at 1.1 Hz frequency. The velocities are plotted across one post constriction, along the cutline in **Figure S2**, at the maximum electric field generated by the applied AC signal for red and green particles, in (A,B) Device ID 4 (C, D) Device ID 5, and (E,F) Device ID 6, respectively.

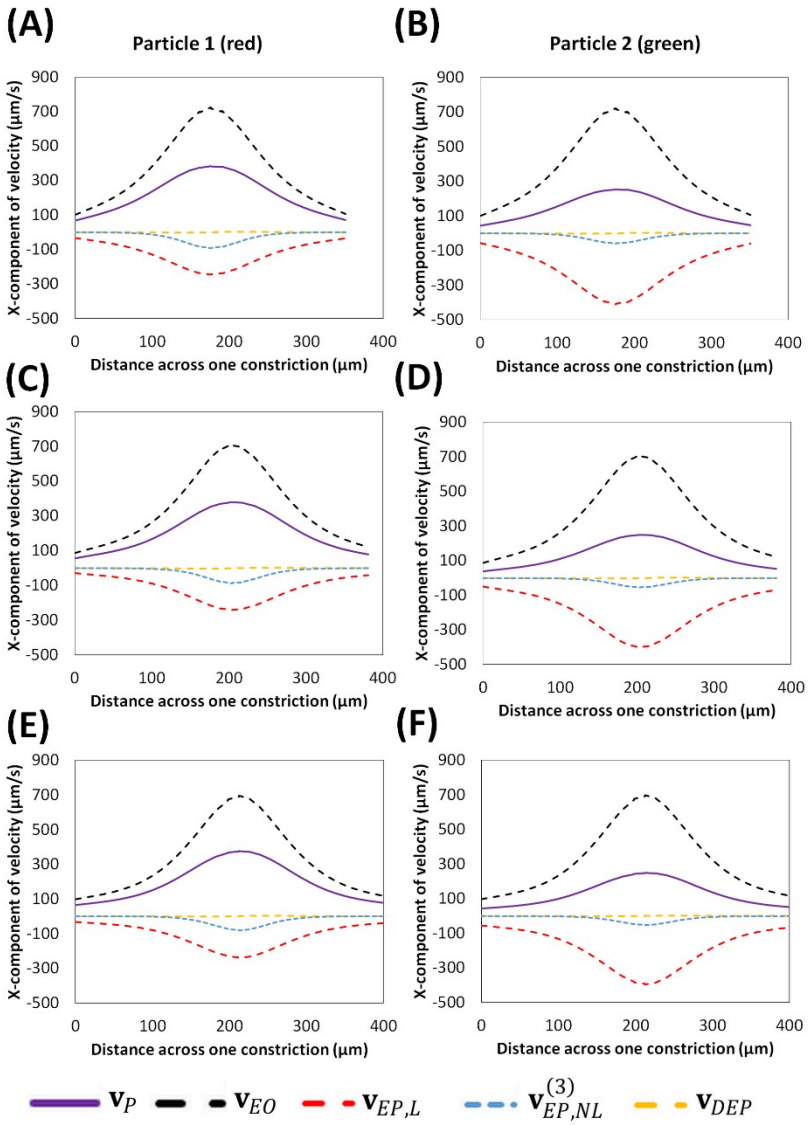

Figure S9. Prediction of the overall and individual particle velocities exerted by the four EK phenomena across a cutline for Device IDs 7-9, by introducing an offset to the post array with VS=35 μm, under 800 V peak amplitude and 300 V DC bias at 1.1 Hz frequency. The predicted velocities are plotted across one post constriction, along the cutline between non-offset posts as shown in **Figure S3**, at the maximum electric field generated by the applied AC signal for red and green particles, in (A,B) Device ID 7 (C, D) Device ID 8, and (E,F) Device ID 9, respectively.

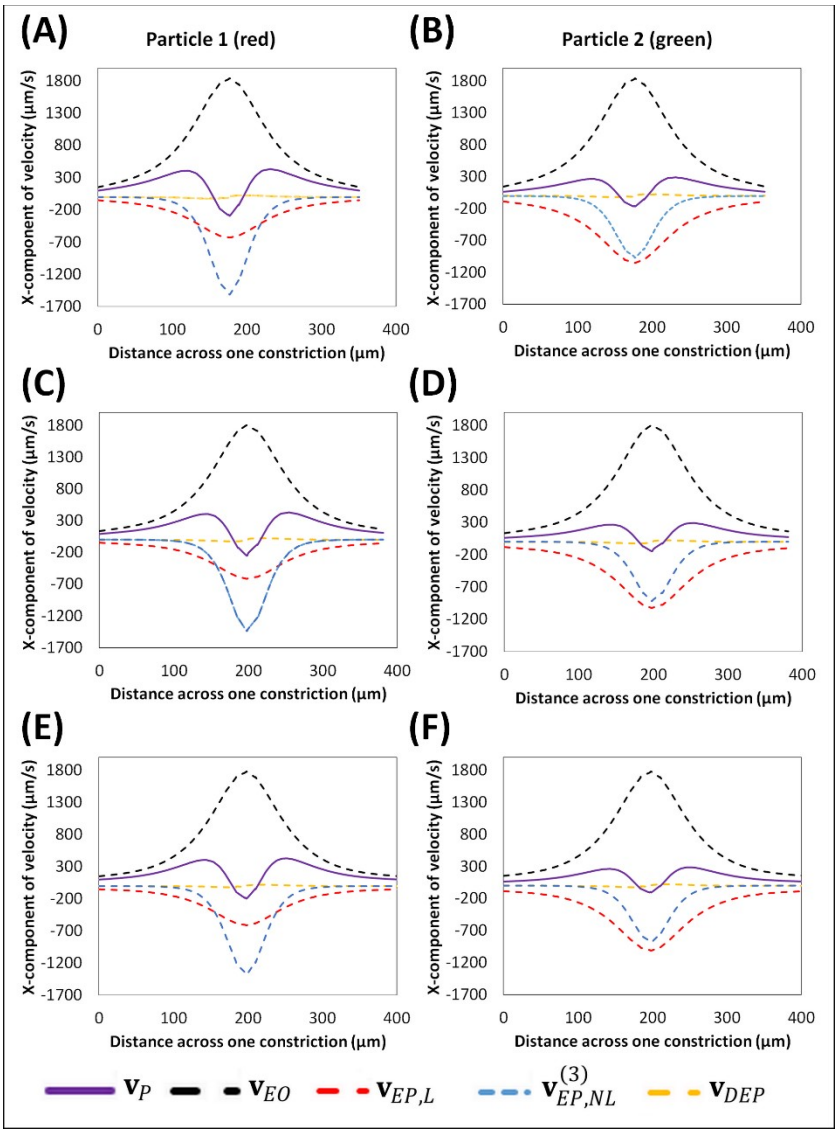

Figure S10. Prediction of the overall and individual particle velocities exerted by the four EK phenomena across a cutline for Device IDs 10-12, by introducing an offset to the post array with VS=18 μm, under 800 V peak amplitude and 300 V DC bias at 1.1 Hz frequency. The predicted velocities are plotted across one post constriction, along the cutline between non-offset posts as shown in **Figure S3**, at the maximum electric field generated by the applied AC signal for red and green particles, in (A,B) Device ID 10 (C, D) Device ID 11, and (E,F) Device ID 12, respectively

References

(1) Schnitzer, O.; Yariv, E. Nonlinear Electrophoresis at Arbitrary Field Strengths: Small-Dukhin-Number Analysis. *Phys. Fluids* **2014**, *26* (12), 122002. https://doi.org/10.1063/1.4902331.

(2) Schnitzer, O.; Zeyde, R.; Yavneh, I.; Yariv, E. Weakly Nonlinear Electrophoresis of a Highly Charged Colloidal Particle. *Phys. Fluids* **2013**, *25* (5), 052004. https://doi.org/10.1063/1.4804672.

(3) Cobos, R.; Khair, A. S. Nonlinear Electrophoretic Velocity of a Spherical Colloidal Particle. *J. Fluid Mech.* **2023**, *968*, A14. https://doi.org/10.1017/jfm.2023.537.

(4) Gallo-Villanueva, R. C.; Perez-Gonzalez, V. H.; Cardenas-Benitez, B.; Jind, B.; Martinez-Chapa, S. O.; Lapizco-Encinas, B. H. Joule Heating Effects in Optimized Insulator-Based Dielectrophoretic Devices: An Interplay between Post Geometry and Temperature Rise. *Electrophoresis* **2019**, *40* (10). https://doi.org/10.1002/elps.201800490.